Heliyon 9 (2023) e20067

Contents lists available at ScienceDirect

Heliyon

journal homepage: www.cell.com/heliyon

Antiviral efficacy of nanomaterial-treated textiles in real-life like exposure conditions☆

Alexandra Nefedova [a], Kai Rausalu [b], Eva Zusinaite [b], Vambola Kisand [a], Mati Kook [a], Krisjanis Smits [c], Alexander Vanetsev [a,**], Angela Ivask [d,*]

[a] Institute of Physics, University of Tartu, W. Ostwaldi Str 1, 50411, Tartu, Estonia
[b] Institute of Technology, University of Tartu, Nooruse 1, 50411, Tartu, Estonia
[c] Institute Solid State Physics, University of Latvia, 8 Kengaraga street, Riga, LV-1063, Latvia
[d] Institute of Molecular and Cell Biology, University of Tartu, Riia 23, 51010, Tartu, Estonia

ARTICLE INFO

Keywords:
Polyester fabric
Nanoparticles
Silicon dioxide
Cerium dioxide
Hexadecyltrimethylammonium bromide
Copper nitrate
Coronavirus
SARS-CoV-2
Antiviral
Virucidal

ABSTRACT

Due to the growing interest towards reducing the number of potentially infectious agents on critical high-touch surfaces, the popularity of antimicrobially and antivirally active surfaces, including textiles, has increased. The goal of this study was to create antiviral textiles by spray-depositing three different nanomaterials, two types of CeO_2 nanoparticles and quaternary ammonium surfactant CTAB loaded SiO_2 nanocontainers, onto the surface of a knitted polyester textile and assess their antiviral activity against two coronaviruses, porcine transmissible gastroenteritis virus (TGEV) and severe acute respiratory syndrome virus (SARS CoV-2). Antiviral testing was carried out in small droplets in semi-dry conditions and in the presence of organic soiling, to mimic aerosol deposition of viruses onto the textiles. In such conditions, SARS CoV-2 stayed infectious at least for 24 h and TGEV infected cells even after 72h of semi-dry deposition suggesting that textiles exhibiting sufficient antiviral activity before or at 24 h, can be considered promising. The antiviral efficacy of nanomaterial-deposited textiles was compared with the activity of the same nanomaterials in colloidal form and with positive control textiles loaded with copper nitrate and CTAB. Our results indicated that after deposition onto the textile, CeO_2 nanoparticles lost most of their antiviral activity, but antiviral efficacy of CTAB-loaded SiO_2 nanocontainers was retained also after deposition. Copper nitrate deposited textile that was used as a positive control, showed relatively high antiviral activity as expected. However, as copper was effectively washed away from the textile already during 1 h, the use of copper for creating antiviral textiles would be impractical. In summary, our results indicated that antiviral activity of textiles cannot be predicted from antiviral efficacy of the deposited compounds in colloid and attention should be paid on prolonged efficacy of antivirally coated textiles.

☆ Angela Ivask reports financial support was provided by Estonian Research Council. Angela Ivask reports financial support was provided by European Commission. Vambola Kisand reports financial support was provided by Estonian Research Council.

* Corresponding author.
** Corresponding author.
E-mail addresses: alexander.vanetsev@ut.ee (A. Vanetsev), angela.ivask@ut.ee (A. Ivask).

https://doi.org/10.1016/j.heliyon.2023.e20067
Received 10 June 2023; Received in revised form 28 August 2023; Accepted 10 September 2023
Available online 12 September 2023

1. Introduction

With the current outbreaks of infectious diseases there has been a significant increase in awareness of the importance of good hygiene practices. Due to the importance of surface transmission in facilitating bacteria or virus-related infectious diseases [1–3], there is a justified interest towards eliminating those microbes from high-touch surfaces, especially those present in common areas. In addition to the disinfection, a feasible solution to decrease the presence of microbes on surfaces would be the use of antibacterial or antiviral coatings or finishes [4,5] either on solid surfaces or on textiles. Indeed, inadequately laundered or disinfected textiles have been often related with healthcare associated infections [6]. Although to date no direct evidence exists that microbe-contaminated textiles had been the cause of large-scale infection outbreaks in hospital settings or in public spaces, adequate control measures should be in place to decrease the presence of potential microbial or viral pathogens on textiles, particularly those used for sensitive population groups [6,7].

Interestingly, despite of significant increase in publications on antiviral compounds during recent years, reports on antiviral surfaces are still relatively scarce. A total of 67 articles were derived with keywords "antivir* coat*" and only 49 with keywords "antivir* surface*" in Clarivate WoS database by January 2023. Compared with antiviral surfaces, even less has been published on antiviral textiles. By January 2023, only 10 papers were present in WoS database for "antivir* textile*" and 8 articles on "antivir* fabric*".

Various compounds and techniques have been used to equip textiles with antiviral properties. Copper and its compounds are probably the most frequently used textile finishings due to their high antiviral efficacy [8]. Antiviral effect was observed for cotton fabric to which copper nanoparticles were deposited by magnetron sputtering [9], for cellulose and polyester textiles with surface-deposited gallium-copper particles [10] and for CuI-based Cu^{+}-ions releasing and reactive oxygen species (ROS) producing thin film created on a textile surface [11]. In addition to copper, also other compounds have been used to create antiviral textiles. ZnO films have been used to coat nanofibrous electrospun silk-polyethylene oxide material for antiviral purposes [12] and ZnO nanoparticles coupled with (3-Glycidoxypropyl) trimethoxysilane have been used to create antiviral cotton fabric [13]. Selenium nanoparticles as part of acrylate-based printing paste have been used to print antiviral polyester fabrics [14] and nano-graphene oxide coating was used in two studies that aimed to prepare antiviral PET textile and linen [15,16]. Also organic antivirals, such as sodium pentaborate, triclosan and glucopon as well as liquid soap formulation have been used to achieve antiviral covering [17,18].

One of the central issue in antiviral textile research is proof of efficacy, which in case of commercialized products is strictly regulated. According to both, European as well as US regulations antiviral surfaces and textiles are required to exhibit at least 3 log decrease in infectious activity within 1–2 h [19–21]. However, based on the current literature, 3 log decrease in viral infectivity has been observed only in case of one of the studied textiles that was coated with sodium pentaborate pentahydrate and triclosan [17]. Interestingly, studies with copper-containing textiles have demonstrated only 1–2 log decrease in viral infectivity. CuI nanoparticles treated textiles decreased the infectivity of SARS-CoV-2 only up to 2.5 logs during 24 h incubation [11], Cu-impregnated cotton decreased the infectious titer of influenza A virus by $\geq$ 2 log during 30 min and other type of Cu-coated textile exhibited only a maximum of 1–2 log decrease in infectivity of vaccinia virus, herpes simplex virus type 1 and influenza A virus H1N1 during 2 h [9]. Most of other nanomaterial-based textiles involving either ZnO, selenium or graphene oxide surface coatings, have shown antiviral activity between 1 and 2 log decrease of infectious units during 1–2 h [12–14,16]. In terms of the duration of exposure, the shortest contact time during which significant (1.5 log) decrease of viral infectivity was observed was 1 min in case of liquid soap treated face masks [18].

It is worth noting that most of the antiviral assays with textiles have been performed in conditions where the viral suspension stock is wetting the textile fully. Mostly ISO 18184 protocol [22], which foresees wetting of 1 g piece of textile with 0.2 mL viral suspension, has been followed [9,10,13]. However, as argued in several opinion articles and critical reviews, testing of antimicrobial efficacy should be carried out in application-relevant settings [23,24] and exposure of virus particles onto a textile in a layer of liquid can rarely be evidenced in real life. Most of the viruses are usually deposited onto surfaces, including textiles, via touch transfer or inside small respiratory droplets [25] which suggests that dry or semi-dry testing would provide more valuable information in terms of application relevancy. In some specific cases, where textiles are designed for filtering purposes, filtering of viral stock through the textile (e.g., in Ref. [16]) can be considered as a good measure for antiviral activity in application-relevant scenarios. Apart from moisture during exposure, also exposure medium may play a critical role in antiviral activity. Yet in most of the studies on antiviral textiles, the exposure medium has been relatively poorly documented. Only some studies define their used test medium, which has been either FBS [15], cell culture medium [16] or bacterial growth medium in case of bacteriophages [18]. Indeed, the presence of organic soiling in antimicrobial testing has been considered as a factor significantly affecting antimicrobial activity results [26]. Therefore, careful consideration of exposure media in antiviral efficacy assays is of utmost importance.

While the testing conditions can be followed from standard procedures, none of the standards limits the maximal amount of active agent on the surface of textiles. However, the use of textiles in practical applications may set limitations to the quantity of active agents, because textile properties, such as elasticity, durability, density, and in many cases even tactual sensations, should not be affected by the treatment. As this aspect is not always considered, it is possible that the practical applicability of some previously suggested antiviral compounds is debatable due to their too high loading on textiles.

In this study, we aimed at developing a nanomaterial-based antiviral treatment for textiles and test such textiles in application-relevant conditions against two coronaviruses, porcine transmissible gastroenteritis virus (TGEV) and severe acute respiratory syndrome virus (SARS CoV-2). CeO_2 NPs, and mesoporous SiO_2 nanocontainers loaded with quaternary ammonium surfactant hexadecyltrimethylammonium bromide (CTAB) were selected as potentially antiviral nanomaterials due to their antiviral properties determined in earlier studies [27,28]. Nanomaterials were sprayed onto polyester textile along with copper nitrate and CTAB that were used as a positive antivirally active control and a control for CTAB-loaded SiO_2 nanocontainers, respectively. Antiviral efficacy of the

textiles was tested in semi-dry conditions in small droplets and in the presence of organic soiling. In order to assess the potential loss of antiviral activity of nanomaterials and compounds after loading to textile surface, the efficacy of textiles was compared with the efficacy of the same nanomaterials and compounds in their colloidal form. To assess the real-life usability of the textiles, their stability was estimated by analyzing leaching of the antiviral components.

2. Materials and methods

Copper (II) nitrate pentahemihydrate (>98%, Sigma-Aldrich), cerium (III) nitrate hexahydrate (99.0%, Sigma-Aldrich), diammonium cerium (IV) nitrate (98%, Fluka), hexamethylenetetramine (HMTA, analytical grade, Sigma-Aldrich), citric acid (99%, Fluka), hexadecyltrimethylammonium bromide (CTAB, 98%, Sigma-Aldrich), tetraethyl orthosilicate (TEOS, 98%, Fluka), ethyl alcohol (analytical grade, Sigma-Aldrich), 30% aqueous ammonia solution (Reagent grade, Sigma Aldrich) were used for chemical synthesis. Cell culture media (DMEM) were from Corning, penicillin (10,000 U/mL), streptomycin (100 μg/mL), and fetal bovine serum (FBS) were from PAN Biotech. Bovine serum albumin (BSA) was from Sigma-Aldrich, yeast extract was from Sigma-Aldrich, carboxymethyl cellulose sodium salt (CMC) and crystal violet were from Thermo Fischer, Tween 20 was from Merck, porcine gastric mucin was from Sigma-Aldrich and phosphate buffered saline (PBS) was made in house according to the general recipe. Soya Casein Digest Lecithin Polysorbate Broth (SCDLP) was prepared using Tryptic Soy Broth (TSB) from BD, Lecithin from Millipore Sigma and Tween 80 from Sigma-Aldrich.For antiviral assays sterile water from B. Braun was used, MQ water was used in all other experiments.

2.1. Synthesis of nanoparticles

NPs of CeO_2 were synthesized as described earlier in our previous article [27]. By using two different synthetic techniques, NPs with positive and negative surface charge were obtained henceforth referred to as CeO_2 (+) and CeO_2 (−).

CeO_2(+) NPs were obtained by hydrolyzing diammonium cerium (IV) nitrate at high temperature in the presence of HMTA. For that, 0.189 g of $(NH_4)_2Ce(NO_3)_6$ and 0.053 g of HMTA were dissolved in 50 mL of water and loaded into an autoclave vessel (100 mL). The vessel was sealed and heated to 180 °C for 30 min in the microwave-hydrothermal device (Berghof Speedwave 4, 2.45 GHz, 1000 W). After thermal treatment, the vessel was cooled down to room temperature in a water bath. The product was centrifuged for 10 min, the sediment was washed with water and redispersed by ultrasonication. These steps were repeated at least 3 times and the final product was redispersed in 5 mL of water by ultrasonication until opalescent pale-yellow colloid was obtained.

For the synthesis of CeO_2(−) NPs, cerium (III) nitrate was hydrolyzed at room temperature in the presence of ammonia with simultaneous oxidation by oxygen from the air. For that, 0.045 g of citric acid was dissolved in 25 mL of prepared in advance 0.05 M aqueous solution of cerium (III) nitrate. The solution was rapidly added into 100 mL of 3 M solution of ammonia and left to stir vigorously for 2 h during which the color of solution changed from colorless to yellow-orange. After that the colloid solution was centrifuged, washed and redispersed by ultrasonication. These steps were repeated at least 3 times and the final product was redispersed in 15 mL of water by ultrasonication until transparent dark yellow colloid was obtained.

Mesoporous SiO_2 nanocontainers loaded with dissolved CTAB, further referred to as CTAB@SiO_2, were synthesized using a modified Stöber technique described in Ref. [29]. For that, 5.2 mL of TEOS, 0.028 g of CTAB, 150 μL of ammonia and 1 mL of water were mixed in 50 mL of ethanol and left at room temperature for 24 h under vigorous stirring. Afterwards, thick white precipitate was separated by centrifugation, washed several times with water and ethanol and dried at 40 °C.

2.2. Characterization of nanomaterials

The mean size of CeO_2 particles and CTAB@SiO_2 nanocontainers was estimated from TEM images (JEOL JEM-2200FS with normal field emission gun, 200 kV acceleration voltage) for which nanomaterials were dispersed in ethanol using ultrasonication and drop casted onto Lacey Carbon Copper TEM grid. Hydrodynamic mean size and ζ-potential were measured in water colloids of 10 mg/L in water using dynamic light scattering (DLS; Malvern Zetasizer instrument). The concentration of component elements in NPs and nanocontainers was measured using elemental analysis by ICP-MS (Agilent 7700 ICP-MS) in case of Ce, Cu, Br and ICP-OES (Agilent 5100 ICP-OES) in case of Si. Br concentration was used to calculate the concentration of CTAB. For ICP measurements true and colloidal solutions were mixed with diluted HNO_3 and directly loaded into the device.

Table 1
Concentrations of antiviral nanomaterials and compounds used to spray the textile.

Antiviral nanomaterial or compound	Concentration in colloid or solution	Textile designation	Purpose of use
CeO_2(+) NPs	21.5 mM	CeO_2(+) textile	Potentially antiviral nanomaterial
CeO_2(−) NPs	27.1 mM	CeO_2(−) textile	Potentially antiviral nanomaterial
SiO_2 nanocontainers loaded with CTAB (CTAB@SiO_2)	215 mM SiO_2 and 0.0013 mM CTAB	CTAB@SiO_2 textile	Potentially antiviral nanomaterial
CTAB	0.005 mM	CTAB textile	Comparison for CTAB@SiO_2
$Cu(NO_3)_2$	62.5 mM	Cu textile	Positive control

2.3. Deposition of nanomaterials onto textile

The used textile was a knitted fabric for mattress covering "Sareaux-C 24" (100% polyester, specific weight 240 g/m^2) provided by TAD Logistics (Estonia). Antiviral compounds (at concentrations indicated in Table 1) were deposited onto the textile by spraying with an air spray nozzle. 15 mL of concentrated solution of the compound or suspension of nanomaterials was sprayed onto 0.0225 m^2 (15 × 15 cm) of vertically placed piece of textile. After spraying, textile pieces were dried at room temperature and textiles were designated as CeO_2(+) textile, CeO_2(−) textile, CTAB@SiO_2 textile, CTAB textile and Cu textile (Table 1). The dried textile was cut to 4 cm^2 pieces (2 × 2 cm squares, mean weight of the piece 0.045 ± 0.008 g), that were further used for antiviral testing, as well as to determine the quantity of deposited material.

2.4. Characterization of antivirally treated textiles

The treated textiles were analyzed for their elemental composition, release of antiviral loading and physical appearance. The concentration of nanomaterials or compounds on textile samples and in their wash-offs (collected samples from antiviral assays; see below) was measured using ICP-MS (Agilent 7700 ICP-MS) in case of Ce, Cu, Br and ICP-OES (Agilent 5100 ICP-OES) for Si. Br concentration was used to calculate the concentration of CTAB as it was safe to consider the absence of any other sources of bromine in samples. To extract the compounds and nanomaterials from textile samples, 0.1 g of textile was placed in 3:1 mixture of HNO_3 and HCl ("reversed aqua regia") and treated using Berghof Speedwave Xpert device until full decomposition. In case of wash-offs the concentration of released nanoparticles and compounds was calculated back to the single 2 × 2 cm textile piece.

Imaging of textile surfaces was performed with SEM (Thermo Fisher Scientific Helios 5 UX device) after fixing the 2 × 2 cm pieces on a sample holder using conductive carbon tape.

2.5. Maintenance and preparation of viruses for antiviral testing

Antiviral assessment was carried out with two coronaviruses, transmissible gastroenteritis virus (TGEV, obtained from prof. L. Enjuanes at Department of Molecular and Cell Biology, National Center of Biotechnology, Madrid, Spain) and severe acute respiratory syndrome virus (SARS-CoV-2, recombinant virus based on the Wuhan-Hu1, MT926410 sequence [30] with S-protein containing amino acid mutations corresponding to the Delta strain).

SARS-CoV-2 was propagated in Vero E6 cells (virus growth medium (VGM) – DMEM supplemented with 0.2% BSA, 100 U/mL penicillin, and 100 μg/mL streptomycin) for 4 days at 37 °C, 5% CO_2. Cell supernatant was collected, clarified by centrifugation at 3000×*g* for 10 min at + 4 °C, aliquoted and stored at −80 °C. The virus titer was determined using immuno-plaque assay as follows: confluent Vero E6 cells on 96-well plates were infected using 25 μL virus dilutions at 37 °C, 5% CO_2, humidified atmosphere for 1 h. Then, ~150 μL of 1% CMC in VGM was added to the plates and incubated further for 48 h at 37 °C, 5% CO_2. The CMC layer was then removed by pipetting, and the cells were fixed using ice-cold 80% acetone/PBS for 1 h, −20 °C. Acetone was removed and plates were dried for at least 3 h. The plates were blocked with 50 μL per well of Pierce™ Clear Milk blocking buffer (Thermo Scientific) for 30 min at 37 °C and after that stained with rabbit anti-SARS-CoV-2-nucleocapsid monoclonal antibody (82C3, ref. R1-179-100, Icosagen, Estonia), following staining with the secondary anti-rabbit IRDye800-conjugated (LI-COR) antibody. The plates were washed with PBS/0.05% Tween 20, dried and scanned using LI-COR Odyssey (LI-COR, USA) device for 800 nm signal; plaques (minimum three plaques per well) were counted from scanned images. At least three independent tests were performed to obtain the resulting titer of 5.73 × 10^5 PFU (plaque forming units) per milliliter.

TGEV was propagated in ST cells (growth medium as above) by incubating the virus-infected cells for 4 days at 37 °C, 5% CO_2. Cell supernatant was collected, clarified by centrifugation at 3000×*g* for 10 min at + 4 °C, filtered through a 0.2 μm filter, aliquoted and stored at −80 °C. The virus titer was determined using plaque assay as follows: 100% confluent ST cells on 12-well plates were infected with 150 μL of virus stock dilutions for 1 h at 37 °C and 5% CO_2 in a humidified atmosphere with gentle rocking every 15 min. The medium was then removed, and 1.5 mL of 1% CMC in VGM was added. Cells were grown for 96 h at 37 °C, 5% CO_2 in a humidified atmosphere. Then, the CMC/VGM was removed, and plates were stained using crystal violet stain and the plaques visually counted. Only wells with at least 3 plaques were considered. At least three independent tests were performed to obtain the resulting titer of 6.33 × 10^7 PFU/mL.

2.6. Antiviral activity assessment

Both, textiles and colloidal or true solutions of active agents were assessed for their antiviral activity.

Antiviral assessment of textiles was carried out essentially following ISO standard 18184 using textile pieces of 2 × 2 cm (0,045 ± 0008 g) that were sterilized by autoclaving. Virus stocks in VGM were mixed 10:1 with 10x soil load (1x soil load: 1 g/L BSA, 1 g/L yeast extract, 0.08 g/L porcine gastric mucin in PBS) [21]. A piece of textile was placed into a 50 mL screw cap tube, ten 2 μL drops of viral stock mixed with soil load were applied to the textile surface and the tube was closed. Viruses were washed off from textiles using 10 mL of SCDLP (30 g/L TSB, 1 g/L lecithin, 7 g/L Tween 80) by vortexing for 5 sec 5 times, at specified timepoints. For 0 h timepoint, virus was washed off from textile immediately. These wash-offs were either directly or after diluting in virus growth medium used to infect the cells for immunoplaque assay or plaque assay as described above. Before counting the plaques, the plates were checked for any cytotoxicity or other interfering effects by visually checking staining of the cell layer. Wells with visual signs of cytotoxicity were not counted. PFU per textile surface was calculated.

Wash-offs from textiles in SCDLP after 10 min UV treatment were also used for elemental analysis by ICP-MS (see section 3.2, Table 3).

In case of "no textile" experiment, similar experimental set-up as in case of textiles was used but no textile was added. Ten 2 μL drops of viral stock mixed with soil load were placed onto the surface of a 50 mL screw cap tube, the tube was closed and viruses were washed using 10 mL of SCDLP at specified timepoints. The resulting virus dilutions were then used to infect cells for immunoplaque or plaque assay.

For antiviral analysis of solutions of nanomaterials or compounds, solutions with different concentrations in water were mixed with equal amount of virus stock was added followed by 1 h incubation at room temperature. The resulting mixtures were further diluted with VGM and used to infect the cells for immunoplaque assay or plaque assay as described above. PFU per ml of compound or nanomaterial was calculated.

Each textile, chemical or nanomaterial concentration was tested at least in three replicates while performing at least three independent experiments. Minimum of three plaques could be reliably counted per one well and this served as a limit of detection (LOD). Results are presented as log PFU/mL for a piece of textile.

2.7. Statistical analysis

Statistically significant differences in antiviral experiments were confirmed by one-way ANOVA analysis for repeated measurements and post-hoc Tukey's range test with CLD output. P-values of less than 0.05 were considered statistically significant.

3. Results and discussion

3.1. Characterization of nanomaterials

Detailed characterization of the ultrasmall, 3.2–3.3 nm diameter CeO_2 NPs was performed in our previous paper [27] and most important parameters are summarized in Table 2. Fig. 1 A and B represent morphology of the synthesized CeO_2 NPs. Synthesized SiO_2 nanocontainers are characterized by the mean size of ~60 nm, spherical shape, and large amount of distinctly visible mesopores with the size around 2–3 nm (Fig. 1C). In case of CTAB loaded into SiO_2 (CTAB@SiO_2), these mesopores are filled with the reaction media of SiO_2 particles synthesis, which was a water-alcohol solution of CTAB. It is also expected that, as a surfactant, CTAB molecules are efficiently adsorbed onto the outer surface of SiO_2 particles, as well as on the inner surface of mesopores. It is expected that in aqueous environment CTAB@SiO_2 will slowly release CTAB due to the concentration gradient.

3.2. Characterization of textiles

General microstructure of the used polyester textile subjected to deposition of nanomaterials is presented on Fig. 2. The textile is knitted of threads with diameter ~400–500 μm, which in their part consist of fibers with diameter ~10 μm. Fibers are densely packed and stranded into threads with large free spaces between.

The two principally different types of nanomaterials loaded onto the polyester textile by spray coating were CeO_2 NPs that according to our previous studies demonstrated antiviral effect in suspension [27], and quaternary ammonium surfactant CTAB-loaded mesoporous SiO_2 (CTAB@SiO_2) that were considered antiviral due to previous studies [31] and because of wide-scale use of CTAB-like compounds in antimicrobial applications. To create a comparative sample for CTAB@SiO_2 textile, CTAB solution alone at approximately the same concentration that it was present in CTAB@SiO_2, was spray coated onto the textile.

In order to prepare a positive control sample with presumably high antiviral activity, the textile was spray coated with $Cu(NO_3)_2$ (Table 1). The active component in resulting Cu textile was expected to be copper ions which are known for their high antiviral activity [8].

The microstructure of untreated and sprayed textile samples is shown in Fig. 3 A-H and the quantity of loadings of active agents on textile in Table 3. Interestingly, the loading efficacy of textile with CeO_2 NPs and CTAB@SiO_2 was very different: CeO_2 could be incorporated to the textile with about 100-fold higher efficacy than CTAB@SiO_2. This could be due to the 20-time size difference between CeO_2 and SiO_2 particles (diameters 3 and 60 nm, respectively) and less efficient attachment of larger particles onto the textile threads. As the textile is composed of polyester lacking any functional groups capable of covalent bonding under the conditions used during spraying, we assume attachment of the particles only due to adhesion to the textile surface – van der Waals forces and weak hydrogen bonding. Therefore, surface/volume ratio of the particles, as well as activity of their surface, play crucial role in their attachment to a thread. And it only can be expected, that smaller particles with more active surface are demonstrating better

Table 2
Main characteristics of synthesized nanoparticles. Mean size of the particles was calculated based on HR TEM data and hydrodynamic mean particle size was determined using DLS analysis.

	CeO_2 (+) NP	CeO_2 (−) NP	CTAB@SiO_2
Mean particle size	3.3 ± 0.4 nm	3.2 ± 0.4 nm	59 ± 14 nm
Hydrodynamic mean particle size	7.0 ± 3.0 nm	4.5 ± 2.0 nm	320 ± 90 nm
ζ-potential	+41 ± 2 mV	−53 ± 4 mV	−29 ± 3 mV

Table 3
Quantities of active compounds on textiles and stability (leaching) of the treated textiles as determined by ICP-MS analysis.

	Active compound on textile, per piece[a]	Active compound in wash-off per piece[a] (% from initial quantity on textile)	
		1 h	24 h
CeO_2(+) textile	8.7 μmol CeO_2	0.014 μmol CeO_2 (0.16%)	0.028 μmol CeO_2 (0.32%)
CeO_2(−) textile	8.7 μmol CeO_2	0.014 μmol CeO_2 (0.16%)	0.028 μmol CeO_2 (0.32%)
CTAB@SiO_2 textile	343 μmol SiO_2 and 0.04 μmol CTAB	0.13 μmol SiO_2 (0.04%) and 0.002 μmol CTAB (5%)	0.14 μmol SiO_2 (0.04%) and 0.002 μmol CTAB (5%)
CTAB textile	0.05 μmol CTAB	0.0015 μmol CTAB (3.5%)[b]	0.0015 μmol CTAB (3.5%)
Cu textile	7.5 μmol $Cu(NO_3)_2$	1.75 μmol $Cu(NO_3)_2$ (23%)	3.75 μmol $Cu(NO_3)_2$ (50%)

[a] 4 cm^2or 0.045 ± 0.008 g textile piece.
[b] Si in wash-off not detected, below limit of detection.

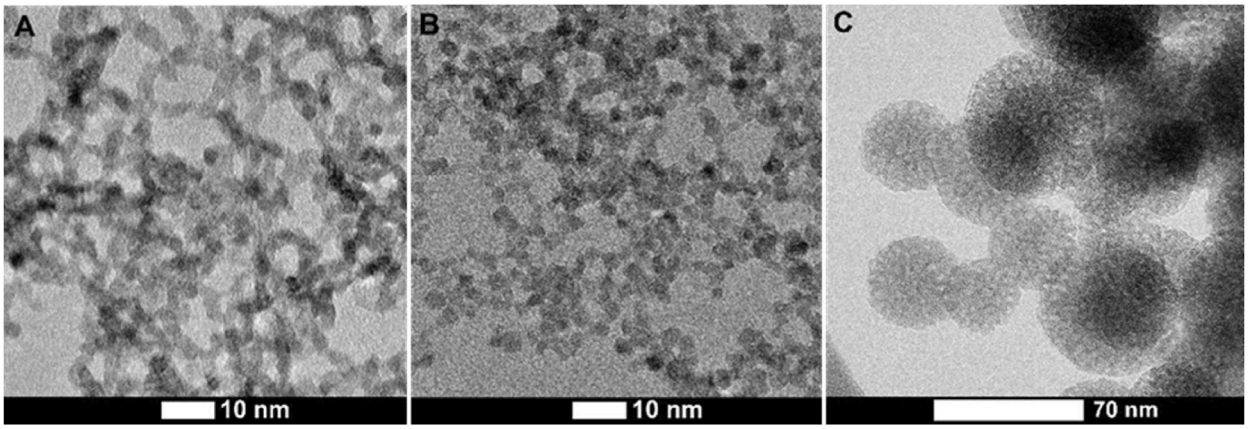

Fig. 1. HR TEM images of synthesized nanomaterials: A - CeO_2(+) NPs, B - CeO_2(−) NPs, C - SiO_2 nanocontainers with CTAB (CTAB@ SiO_2).

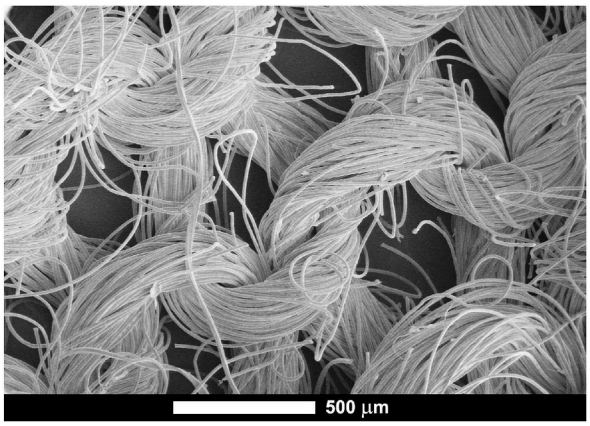

Fig. 2. SEM microphotograph of the untreated textile at low magnification.

attachment. Also, from SEM images it can be seen that smaller CeO_2 particles form a continuous layer on the fiber surface (Fig. 3C–F), while larger SiO_2 nanocontainers tend to form "islands" probably due to stronger aggregation in the initial colloid (Fig. 3 G, H)).

In order to study the stability of the textiles, we measured the release of active components from treated textiles under the simulated conditions of an antiviral assay. The release profiles of potentially antiviral compounds from textile surfaces were notably different and dependent on the chemical nature of the deposited material (Table 3). The highest release from textiles was observed for Cu textile in which case after 1 h 23% of the initial $Cu(NO_3)_2$ loading was released and after 24 h 50% of the loading was leached out. On the other hand, the level of CeO_2 NPs release was negligible (0.16%) and according to existing data on CeO_2 low solubility [32], this release was probably only due to detachment of NPs from textile surface. Interestingly, the level of CTAB release from CTAB textile surface was relatively low, reaching only 3.5% of the initial loading. It was also surprising that CTAB release from CTAB@SiO_2 textile was comparable with that of CTAB textile (Table 3). Theoretically encapsulation of CTAB in SiO_2 mesopores could ensure a slow but

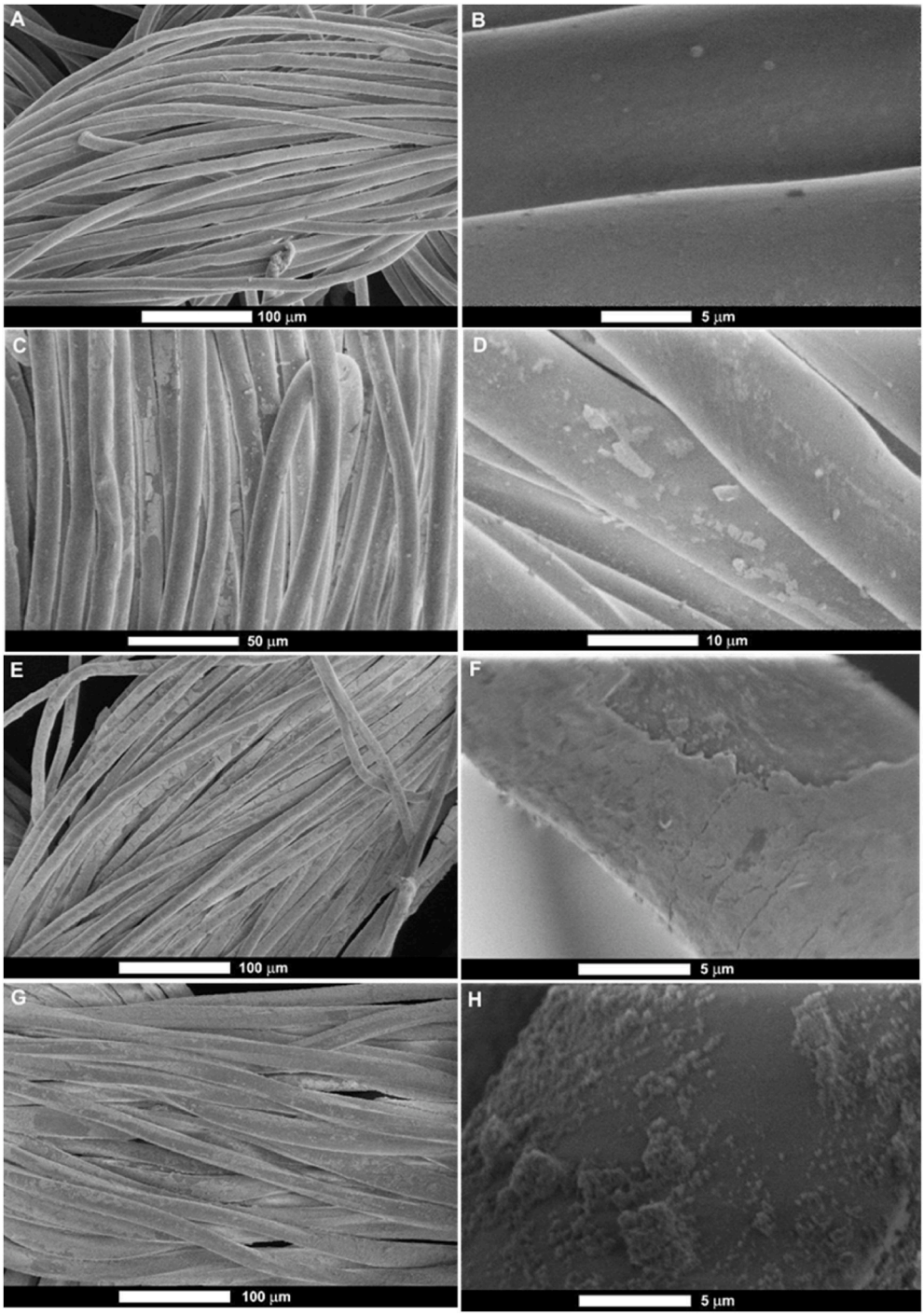

Fig. 3. SEM images of textiles sprayed with nanomaterials. (A–B) untreated textile, (C–D) $CeO_2(+)$ textile (E–F) $CeO_2(-)$ textile, (G–H) CTAB@-SiO_2 textile.

continuous release of CTAB. Therefore, we suggest that the first wash-off of CTAB that was analyzed in our release assay was most likely determined by the rate at which SiO_2 surface-attached CTAB was released and CTAB "hidden" in mesopores did not release with this first burst. In case of CTAB@SiO_2 textile is also noticeable an extremely low content of SiO_2 in the wash-offs (0.04% of the initial load on textile), which proves that SiO_2 nanocontainers were relatively tightly bound to the textile surface. Based on those findings we can conclude that textiles loaded with soluble copper salts such as $Cu(NO_3)_2$ are unstable and non-resistant to any wet treatments or moist environment and longer-lasting applications. At the same time, nanomaterial treatments on textiles are more stable and less

prone to release the active components. However, the nanomaterial loadings used in this work are probably excessive for real-life application of textile materials and e.g., in case of CeO_2 treatment the color of textile was visibly changed to yellowish. On the other hand, the physical properties of CTAB@SiO_2 textile did not visibly change compared with untreated textile. Interestingly though, CTAB textile on which CTAB was added at approximately the same concentration as in CTAB@SiO_2, turned "soapy" by the touch. Considering that treatment of textiles should minimally change the visual appearance or tactual sensations, CTAB@SiO_2 surface treatment could be proposed as a promising candidate for future developments, in case of its sufficient antiviral activity.

3.3. Antiviral efficacy of textiles

For antiviral efficacy assessment, two coronaviruses, porcine transmissible gastroenteritis virus (TGEV), which can be considered as a model coronavirus transmitting through the fecal-oral route, and severe acute respiratory syndrome virus SARS-CoV-2 that can be considered as a model virus transmitting through respiratory route, were selected. In order to place the antiviral efficacy data of textiles into the context, all nanomaterials and compounds loaded onto the textiles were also assessed for their antiviral activity in their solution form (Fig. 4). Overall, the sensitivity profiles of TGEV and SARS-CoV-2 towards the tested compounds at 1 h exposure were relatively similar. Among the tested compounds CTAB was effective at lowest concentrations, but when loaded to mesopores of SiO_2 in CTAB@SiO_2, lost significantly in its antiviral efficacy. Interestingly, CeO_2 NPs and $Cu(NO_3)_2$ showed antiviral efficacy at relatively similar concentrations, between 0.1 and 1 mM (Fig. 4 A and B).

Although the sensitivity profile of both viruses was generally similar, some small differences were observed. Compared with SARS-CoV-2, TGEV was inhibited by lower concentrations of CTAB (one log decrease in PFU obtained at about 0.002 mM in case of TGEV and 0.01 in case of SARS-CoV-2). Similarly, CTAB@SiO_2 did not affect SARS-CoV-2, but at highest CTAB concentration decreased the PFU of TGEV virus by about 1 log (Fig. 4 A). Higher sensitivity of TGEV towards CTAB was somewhat surprising but may be explained by potentially higher concentration of cholesterol in the lipid membrane of this virus [33] compared with SARS-CoV-2, which membrane contains more phospholipids with little representation of cholesterol or sphingolipids [34]. As cholesterol provides high negative charge to lipid membranes [35] enabling to attract more cationic CTAB [36], such a difference between the surfaces of those viruses may cause the differences in sensitivity profiles towards cationic compounds. On the other hand, CTAB at higher concentrations was still effective towards SARS-CoV-2 (Fig. 4 B) as also demonstrated in a recent study by Guerrero-Bermea et al. [37].

Before testing the antiviral efficacy of treated textiles, survival experiments of TGEV and SARS-CoV-2 on untreated (control) textile was carried out in order to determine the meaningful duration for the antiviral test and to put the following antiviral efficacy data into the context. Previous reports have shown that the residence time of viruses on textiles can be relatively long on cotton and silk, and the survival time varies between 1 day up to 7 months [38]. Also, temperature has been shown to affect the virus survival on surfaces, in that at lower temperatures the viruses seem to survive more efficiently [38]. On our textile, the selected coronaviruses survived well during 1 h semi-dry exposure at room temperature. Also, after 24 h exposure, the number of TGEV PFU was not significantly different from the initial viral loading (Fig. 5A). Apparently, SARS-CoV-2 was more prone to drying and PFU of this virus decreased for about 1.5 log after 24 h of semi-dry exposure. This decrease was however similar to the decrease of PFU in semi-dry conditions without textile (Fig. 5B) and thus, was caused by simple drying and not due to any specific interactions between the virus and the textile surface. After 48 h of semi-dry exposure however, on textile surface most of SARS-CoV-2 infectious particles were inactivated, whereas in no textile experiment, 4 logs of PFU were remaining (Fig. 5B). After 72 h, all infectious SARS-CoV-2 particles were lost both, on textile as well as without textile. In case of TGEV, 48 h of semi-dry exposure decreased the number of infectious particles by about 1 log and only after 72 h on non-treated textile around 2 logs of infectivity was lost (Fig. 5A). These time-course virus survival experiments demonstrate that in general, antiviral compounds having an effect before 48 h of exposure could be considered useable. In case of TGEV, also antiviral treatments that would be active at or after 72 h could be used. Based on this result and suggestions in standard methods (e.g.,

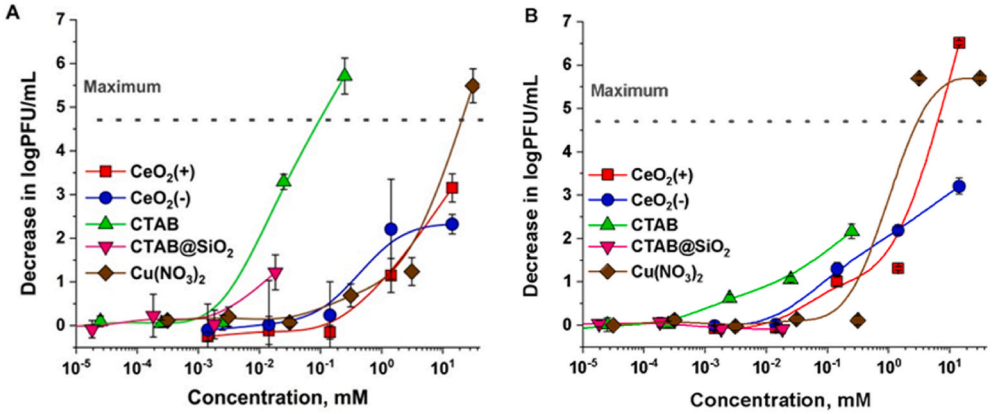

Fig. 4. Effect of NP solutions or solutions of compounds on two coronaviruses, TGEV (A) and SARS-CoV-2 (B). The average decrease in log plaque forming units (PFU)/mL from at least three independent experiments with standard deviation is shown. Dotted line represents maximum decrease in log PFU/mL that could be reliably shown.

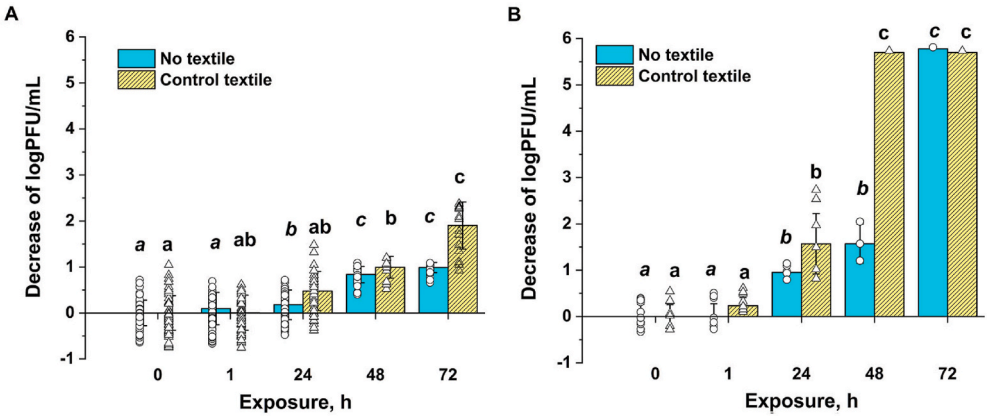

Fig. 5. Infectivity of TGEV (A) and SARS-CoV-2 (B) expressed as log plaque forming units (PFU)/mL after semi-dry exposure to untreated textile or in a similar exposure without textile during 1–72 h. Lower case letters indicate statistically independent groups, as according to Tukey range test with P-value <0.05.

ISO 18184), we exposed TGEV and SARS-CoV-2 viruses to the treated textiles for 1 and 24 h and compared the PFU counts on those test textiles with PFU counts on non-treated textiles at those timepoints.

Antiviral effect data on treated textiles after 0, 1 and 24 h exposure is shown in Fig. 6. Clearly the most antivirally effective was Cu textile that exhibited notable (>3 log decrease in PFU) antiviral activity already after 1 h of exposure, i.e., in case of short-time exposure scenario. After 24 h of exposure, i.e., a long-term exposure scenario, Cu textile decreased the infective viral counts on textile already by 4 logs. However, as discussed above, the results from stability and leaching experiments (Table 3) clearly indicated very effective release of copper from Cu textile and thus, such textiles could be recommended only for short periods in relatively dry conditions.

Although $Cu(NO_3)_2$ and CeO_2 showed relatively similar antiviral profile when tested in solution (Fig. 4), their effect on textile was very different; Cu textile showed very strong antiviral activity whereas no notable antiviral activity was observed for CeO_2 textile. It is important to mention that comparison of Cu and CeO_2 textiles in terms of their antiviral activity is justified due to their similar loadings on textiles (7.5 μmol of $Cu(NO_3)_2$ and 8.7 μmol of CeO_2 per piece; Table 3). It is proposed that the high antiviral effect of Cu textiles was driven by efficient leaching of copper from this textile whereas CeO_2 textile did not release any traceable amounts of the active NPs. This suggests that effective antiviral textiles may be obtained only in case sufficient amount of active agents will be released from the textile surfaces whereas the antiviral activity of surface-attached agents remains relatively low.

In addition to Cu textile CTAB@SiO_2 was the other textile demonstrating antiviral activity, however at significant (>3 log decrease in PFU) levels only after 24 h of exposure, i.e., in long-term exposure scenario. In case of SARS-CoV-2, CTAB@SiO_2 textiles showed a similar effect to CTAB textiles (Fig. 6B). Considering similar level of release of CTAB from both CTAB@SiO_2 as well as CTAB textiles (Table 3), the expected antiviral efficacy of those textiles could be indeed similar. Interestingly however, TGEV was less affected by CTAB textile than by CTAB@SiO_2 textile (Fig. 6A). Therefore, considering the efficacy of CTAB@SiO_2 textiles against both of the tested viruses and relative stability of the CTAB@SiO_2 textile due to low level of SiO_2 and CTAB leaching (Table 3), such a textile would have a clear potential for antiviral use.

Interestingly, earlier studies on antiviral textiles have not attempted to address the issue with potential loss of antiviral activity of their active compounds after loading onto textiles. In our study we were able to only broadly compare the efficacy of antiviral compounds before and after textile loading due several uncertainties, including potential variation in contact area between virus and surface and spatial differences in textile loadings. However, as already indicated, our results showed that compounds not dissolving or releasing from textile surfaces have generally lower antiviral activity than those showing fast dissolution profiles. Another possibility for low antiviral activity of e.g., CeO_2 textiles could be potential masking of ultrasmall NPs by the textile and their non-availability to viruses. However, our results on CTAB and CTAB@SiO_2 textiles suggest that the change in antiviral activity is not simply partial "surface masking" but is more complicated and sensitive to the nature of antiviral material. For example, in solution, CTAB was clearly more efficient towards both coronaviruses than after its loading to SiO_2 nanocontainers in the form of CTAB@SiO_2 (Fig. 4). On the other hand, on textile after 1 h of exposure the antiviral effect of CTAB and CTAB@SiO_2 were comparable while after 24 h exposure CTAB@SiO_2 showed even significantly higher antiviral activity towards SARS-CoV-2. This result requires further investigation; however, we may suggest that in semi-dry conditions the amount of intrinsic moisture in the antiviral material becomes important. Aqueous CTAB entrapped in SiO_2 mesoporous nanocontainers during their preparation (about 50% of particle weight by our rough estimation) is irrelevant in case of colloidal experiments, but becomes crucial on the textile surface, as it allows partial dissolution of CTAB in the conditions of severe deficiency of solvent. This hypothesis allows to explain also the crucial decrease in antiviral activity of CeO_2 nanoparticles when moving from colloids to textile surface. Due to high degree of crystallinity these particles contain very small amount of intrinsic moisture. $Cu(NO_3)_2$ shows reasonable activity even in semi-dry conditions, but this can be explained by its extremely good solubility and high hygroscopicity.

In a wider context these results put forward an important problem for antiviral treatment of textiles. As shown by us and other

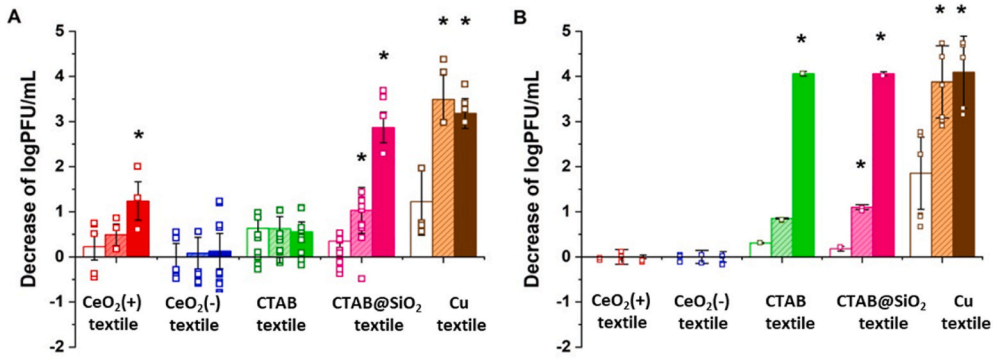

Fig. 6. Decrease in log plaque forming units (PFU)/mL of TGEV (A) and SARS-CoV-2 (B) on treated textiles as compared with control non-treated textile at the same time point. White-out columns represent 0 h exposure, light colored and textured – 1 h exposure and dark colored – 24 h exposure. The results that are statistically different from the corresponding control textiles according to Tukey range test with P-value <0.05 are marked with asterisk.

authors earlier, viruses may survive a rather long time in relatively dry conditions and therefore, antiviral compounds should be able to deactivate viruses even under very low humidity. However, many popular inorganic antiviral agents (copper and silver metal nanoparticles, zinc, titanium and copper oxide nanoparticles, etc.) are efficient only in presence of water, but contain very small if any intrinsic moisture. Thus, these compounds will most likely not be efficient in dry or semi-dry conditions. Nanocontainers, on the other hand, in a form of porous inorganic or polymeric nanoparticles, hydrogels, activated carbon, etc., are capable of containing significant amount of internal moisture. This opens a perspective for their usage in the antiviral treatment of textiles, that are not in direct contact with water and are operated in normal or low humidity conditions.

4. Conclusions

In this study, three types of nanomaterials, two forms of ultrasmall CeO_2 nanoparticles and CTAB-loaded SiO_2 nanocontainers (CTAB@SiO_2) were spray-deposited onto the surface of polyester textile with a goal to equip the textile with antiviral properties. Antiviral efficacy of the resulting treated textiles was assessed against two coronaviruses, porcine transmissible gastroenteritis virus TGEV and SARS-CoV-2 in semi-dry conditions and in the presence of organic soiling. In parallel, antiviral efficacy of the used nanomaterials was also measured in colloidal form. Compared with their activity in colloid, the antiviral efficacy of nanomaterials decreased after their deposition onto the textile surface. Deposition of CeO_2 NPs onto the textile surface totally abolished their antiviral effect, likely due to extremely low solubility and "surface masking" inhibiting the direct contact between viruses and surface deposited NPs. CTAB@SiO_2 retained a higher portion of its activity on textile and CTAB@SiO_2 textile exhibited significant antiviral efficacy after 1 and 24 h of exposure. Considering also the relative stability and low leachability of SiO_2 and CTAB from the loaded textile as well as preservation of physical characteristics of the textile after CTAB@SiO_2 loading, CTAB@SiO_2 nanomaterials could be considered as a promising antiviral treatment for textiles and surfaces to be used in dry and semi-dry conditions. We also demonstrated that despite of immediate high antiviral activity, $Cu(NO_3)_2$ loaded textile surfaces that were used as a positive control, could not be considered for practical use due to the changes in physical appearance of the textile as well as efficient leaching of copper ions in moist conditions. Therefore, when designing antivirally effective surface coatings, antiviral efficacy in application-relevant conditions, durability and stability as well as physical appearance should be considered.

Author contribution statement

Alexandra Nefedova: Performed the experiments, Analyzed and interpreted the data, Wrote the paper.
Kai Rausalu: Performed the experiments, Analyzed and interpreted the data.
Eva Zusinaite: Performed the experiments, Conceived and designed the experiments.
Vambola Kisand: Conceived and designed the experiments, Wrote the paper.
Mati Kook: Performed the experiments, Contributed reagents, materials, analysis tools or data.
Krisjanis Smits: Performed the experiments, analyzed and interpreted the data.
Alexander Vanetsev: Conceived and designed the experiments, Analyzed and interpreted the data, Wrote the paper.
Angela Ivask: Conceived and designed the experiments, Analyzed and interpreted the data, Wrote the paper.

Declaration of competing interest

The authors declare the following financial interests/personal relationships which may be considered as potential competing interests.

Acknowledgements

We thank the following people and institutions for their contribution to our investigation. Toomas Varjund from TAD Logistics OÜ for providing the textiles. Ülis Sõukand from Estonian Environmental Research Center for his help with methods of chemical analysis. Estonian Research Council projects COVSG2, PRG629, PRG1496, PRG1154 and European Commission project STOP (Grant agreement ID: 101057961) for their financial support. The Center of nanomaterials technologies and research (NAMUR+) for core facility funded by project TT13 which was used conducting the research.

References

[1] National Center for Immunization and Respiratory Diseases (NCIRD), Division of Viral Diseases, 2020-. Science Brief: SARS-CoV-2 and Surface (Fomite) Transmission for Indoor Community Environments, CDC COVID-19 Science Briefs, Centers for Disease Control and Prevention (US), Atlanta (GA), 2020 [Internet].
[2] D.-T. Chu, V. Singh, S.-M. Vu Ngoc, T.-L. Nguyen, D. Barceló, Transmission of SARS-CoV-2 infections and exposure in surfaces, points and wastewaters: a global one health perspective, Case Studies in Chemical and Environmental Engineering 5 (2022), 100184, https://doi.org/10.1016/j.cscee.2022.100184.
[3] P. Vasickova, I. Pavlik, M. Verani, A. Carducci, Issues concerning survival of viruses on surfaces, Food Environ Virol 2 (1) (2010) 24–34, https://doi.org/10.1007/s12560-010-9025-6.
[4] K. Shirvanimoghaddam, M.K. Akbari, R. Yadav, A.K. Al-Tamimi, M. Naebe, Fight against COVID-19: the case of antiviral surfaces, Apl. Mater. 9 (3) (2021), 031112, https://doi.org/10.1063/5.0043009.
[5] Z. Sun, K. Ostrikov, Ken), Future antiviral surfaces: lessons from COVID-19 pandemic, Sustainable Materials and Technologies 25 (2020), e00203, https://doi.org/10.1016/j.susmat.2020.e00203.
[6] L. Owen, K. Laird, The role of textiles as fomites in the healthcare environment: a review of the infection control risk, PeerJ 8 (2020), e9790, https://doi.org/10.7717/peerj.9790.
[7] R.W. Sidwell, G.J. Dixon, Role of virucides in controlling virus dissemination by fabrics, J. Am. Oil Chem. Soc. 46 (10) (1969) 532–536, https://doi.org/10.1007/BF02633177.
[8] V. Govind, S. Bharadwaj, M.R. Sai Ganesh, J. Vishnu, K.V. Shankar, B. Shankar, R. Rajesh, Antiviral properties of copper and its alloys to inactivate covid-19 virus: a review, Biometals 34 (6) (2021) 1217–1235, https://doi.org/10.1007/s10534-021-00339-4.
[9] M. Cieślak, D. Kowalczyk, M. Krzyżowska, M. Janicka, E. Witczak, I. Kamińska, Effect of Cu modified textile structures on antibacterial and antiviral protection, Materials 15 (17) (2022) 6164, https://doi.org/10.3390/ma15176164.
[10] K.Y. Kwon, S. Cheeseman, A. Frias-De-Diego, H. Hong, J. Yang, W. Jung, H. Yin, B.J. Murdoch, F. Scholle, N. Crook, E. Crisci, M.D. Dickey, V.K. Truong, T. Kim, A liquid metal mediated metallic coating for antimicrobial and antiviral fabrics, Adv. Mater. 33 (45) (2021), 2104298, https://doi.org/10.1002/adma.202104298.
[11] Y. Takeda, D. Jamsransuren, T. Nagao, Y. Fukui, S. Matsuda, H. Ogawa, Application of copper iodide nanoparticle-doped film and fabric to inactivate SARS-CoV-2 via the virucidal activity of cuprous ions (Cu^{+}), 21, Appl. Environ. Microbiol. 87 (24) (2021), e01824, https://doi.org/10.1128/AEM.01824-21.
[12] U. Kumar, C.R. Fox, C. Feit, E. Kolanthai, J. Sheiber, Y. Fu, S. Singh, P. Banerjee, G.D. Parks, S. Seal, ALD based nanostructured zinc oxide coated antiviral silk fabric, RSC Adv. 12 (30) (2022) 19327–19339, https://doi.org/10.1039/D2RA02653H.
[13] F. Afzal, M. Ashraf, S. Manzoor, H. Aziz, A. Nosheen, S. Riaz, Development of novel antiviral nanofinishes for bioactive textiles, Polym. Bull. (2022), https://doi.org/10.1007/s00289-022-04461-2.
[14] T. Abou Elmaaty, K. Sayed-Ahmed, H. Elsisi, S.M. Ramadan, H. Sorour, M. Magdi, S.A. Abdeldayem, Novel antiviral and antibacterial durable polyester fabrics printed with selenium nanoparticles (SeNPs), Polymers 14 (5) (2022) 955, https://doi.org/10.3390/polym14050955.
[15] A.J. Galante, K.A. Yates, E.G. Romanowski, R.M.Q. Shanks, P.W. Leu, Coal-derived functionalized nano-graphene oxide for bleach washable, durable antiviral fabric coatings, ACS Appl. Nano Mater. 5 (1) (2022) 718–728, https://doi.org/10.1021/acsanm.1c03448.
[16] F. Valentini, M. Cirone, M. Relucenti, R. Santarelli, A. Gaeta, V. Mussi, S. De Simone, A. Zicari, S. Mardente, Antiviral filtering capacity of GO-coated textiles, Appl. Sci. 11 (16) (2021) 7501, https://doi.org/10.3390/app11167501.
[17] Z.U. Iyigundogdu, O. Demir, A.B. Asutay, F. Sahin, Developing novel antimicrobial and antiviral textile products, Appl. Biochem. Biotechnol. 181 (3) (2017) 1155–1166, https://doi.org/10.1007/s12010-016-2275-5.
[18] A. Cano-Vicent, A. Tuñón-Molina, M. Martí, Y. Muramoto, T. Noda, K. Takayama, Á. Serrano-Aroca, Antiviral face mask functionalized with solidified hand soap: low-cost infection prevention clothing against enveloped viruses such as SARS-CoV-2, ACS Omega 6 (36) (2021) 23495–23503, https://doi.org/10.1021/acsomega.1c03511.
[19] The Biocidal Products Regulation - Treated Articles, 2012. https://echa.europa.eu/regulations/biocidal-products-regulation/treated-articles.
[20] Appendix 1 BPR efficacy working, Group Document 1 (39) (2022) 2022. November.
[21] Standard Operating Procedure for OECD Quantitative Method for Evaluating Bactericidal and Mycobactericidal Activity of Microbicides Used on Hard, Non-Porous Surfaces, 2019. https://www.epa.gov/sites/default/files/2019-05/documents/mb-25-05.pdf.
[22] ISO Standard 18184:2019, Textiles — Determination of Antiviral Activity of Textile Products, https://www.iso.org/standard/71292.html, 2019.
[23] X. Song, J. Padrão, A.I. Ribeiro, A. Zille, Testing, characterization and regulations of antimicrobial textiles, in: Antimicrobial Textiles from Natural Resources, The Textile Institute Book Series; Elsevier, 2021, pp. 485–511, https://doi.org/10.1016/B978-0-12-821485-5.00012-3.
[24] E. Pinho, L. Magalhães, M. Henriques, R. Oliveira, Antimicrobial activity assessment of textiles: standard methods comparison, Ann. Microbiol. 61 (3) (2011) 493–498, https://doi.org/10.1007/s13213-010-0163-8.
[25] S. Behzadinasab, A.W.H. Chin, M. Hosseini, L.L.M. Poon, W.A. Ducker, SARS-CoV-2 virus transfers to skin through contact with contaminated solids, Sci. Rep. 11 (1) (2021), 22868, https://doi.org/10.1038/s41598-021-00843-0.
[26] A.J. Cunliffe, P.D. Askew, I. Stephan, G. Iredale, P. M Cosemans, L.M. Simmons, J. Verran, J. Redfern, How do we determine the efficacy of an antibacterial surface? A review of standardised antibacterial material testing methods, Antibiotics 10 (9) (2021) 1069, https://doi.org/10.3390/antibiotics10091069.
[27] A. Nefedova, K. Rausalu, E. Zusinaite, A. Vanetsev, M. Rosenberg, K. Koppel, S. Lilla, M. Visnapuu, K. Smits, V. Kisand, T. Tätte, A. Ivask, Antiviral efficacy of cerium oxide nanoparticles, Sci. Rep. 12 (1) (2022), 18746, https://doi.org/10.1038/s41598-022-23465-6.
[28] M.H. Ly-Chatain, S. Moussaoui, A. Vera, V. Rigobello, Y. Demarigny, Antiviral effect of cationic compounds on bacteriophages, Front. Microbiol. 4 (2013), https://doi.org/10.3389/fmicb.2013.00046.
[29] X. Liu, X. Lu, P. Wen, X. Shu, F. Chi, Synthesis of ultrasmall silica nanoparticles for application as deep-ultraviolet antireflection coatings, Appl. Surf. Sci. 420 (2017) 180–185, https://doi.org/10.1016/j.apsusc.2017.05.124.
[30] S.J. Rihn, A. Merits, S. Bakshi, M.L. Turnbull, A. Wickenhagen, A.J.T. Alexander, C. Baillie, B. Brennan, F. Brown, K. Brunker, S.R. Bryden, K.A. Burness, S. Carmichael, S.J. Cole, V.M. Cowton, P. Davies, C. Davis, G. De Lorenzo, C.L. Donald, M. Dorward, J.I. Dunlop, M. Elliott, M. Fares, A. da Silva Filipe, J. R. Freitas, W. Furnon, R.J. Gestuveo, A. Geyer, D. Giesel, D.M. Goldfarb, N. Goodman, R. Gunson, C.J. Hastie, V. Herder, J. Hughes, C. Johnson, N. Johnson, A. Kohl, K. Kerr, H. Leech, L.S. Lello, K. Li, G. Lieber, X. Liu, R. Lingala, C. Loney, D. Mair, M.J. McElwee, S. McFarlane, J. Nichols, K. Nomikou, A. Orr, R. J. Orton, M. Palmarini, Y.A. Parr, R.M. Pinto, S. Raggett, E. Reid, D.L. Robertson, J. Royle, N. Cameron-Ruiz, J.G. Shepherd, K. Smollett, D.G. Stewart, M. Stewart, E. Sugrue, A.M. Szemiel, A. Taggart, E.C. Thomson, L. Tong, L.S. Torrie, R. Toth, M. Varjak, S. Wang, S.G. Wilkinson, P.G. Wyatt, E. Zusinaite, D. R. Alessi, A.H. Patel, A. Zaid, S.J. Wilson, S. Mahalingam, A plasmid DNA-launched SARS-CoV-2 reverse genetics system and coronavirus toolkit for COVID-19 research, PLoS Biol. 19 (2) (2021), e3001091, https://doi.org/10.1371/journal.pbio.3001091.

[31] C.L. Schrank, K.P.C. Minbiole, W.M. Wuest, Are quaternary ammonium compounds, the workhorse disinfectants, effective against severe acute respiratory syndrome-coronavirus-2? ACS Infect. Dis. 6 (7) (2020) 1553–1557, https://doi.org/10.1021/acsinfecdis.0c00265.
[32] T.V. Plakhova, A.Y. Romanchuk, S.N. Yakunin, T. Dumas, S. Demir, S. Wang, S.G. Minasian, D.K. Shuh, T. Tyliszczak, A.A. Shiryaev, A.V. Egorov, V.K. Ivanov, S. N. Kalmykov, Solubility of nanocrystalline cerium dioxide: experimental data and thermodynamic modeling, J. Phys. Chem. C 120 (39) (2016) 22615–22626, https://doi.org/10.1021/acs.jpcc.6b05650.
[33] X. Ren, J. Glende, J. Yin, C. Schwegmann-Wessels, G. Herrler, Importance of cholesterol for infection of cells by transmissible gastroenteritis virus, Virus Res. 137 (2) (2008) 220–224, https://doi.org/10.1016/j.virusres.2008.07.023.
[34] Z. Saud, V.J. Tyrrell, A. Zaragkoulias, M.B. Protty, E. Statkute, A. Rubina, K. Bentley, D.A. White, P.D.S. Rodrigues, R.C. Murphy, H. Köfeler, W.J. Griffiths, J. Alvarez-Jarreta, R.W. Brown, R.G. Newcombe, J. Heyman, M. Pritchard, R.W.J. Mcleod, A. Arya, C.-A. Lynch, D. Owens, P.V. Jenkins, N.J. Buurma, V. B. O'Donnell, D.W. Thomas, R.J. Stanton, The SARS-CoV2 envelope differs from host cells, exposes procoagulant lipids, and is disrupted in vivo by oral rinses, JLR (J. Lipid Res.) 63 (6) (2022), 100208, https://doi.org/10.1016/j.jlr.2022.100208.
[35] M. Doktorova, F.A. Heberle, R.L. Kingston, G. Khelashvili, M.A. Cuendet, Y. Wen, J. Katsaras, G.W. Feigenson, V.M. Vogt, R.A. Dick, Cholesterol promotes protein binding by affecting membrane electrostatics and solvation properties, Biophys. J. 113 (9) (2017) 2004–2015, https://doi.org/10.1016/j.bpj.2017.08.055.
[36] D.B. Vieira, Cationic lipids and surfactants as antifungal agents: mode of action, J. Antimicrob. Chemother. 58 (4) (2006) 760–767, https://doi.org/10.1093/jac/dkl312.
[37] C. Guerrero-Bermea, N. Rodríguez Fuentes, J.M. Cervantes-Uc, L.E. Alcántara Quintana, F. Díaz-Barriga, F. Pérez-Vázquez, K. González-Palomo, J.A. Uribe-Calderon, Antiviral capacity of polypropylene/(1-hexadecyl) trimethyl-ammonium bromide composites against COVID-19, Polym. Eng. Sci. 62 (12) (2022) 4129–4135, https://doi.org/10.1002/pen.26172.
[38] G. Kampf, How long can nosocomial pathogens survive on textiles? A systematic review, GMS Hyg Infect Control 15 (2020) Doc10, https://doi.org/10.3205/dgkh000345.